

## The Apollo 15 Lunar Samples: A Preliminary Description

Apollo 15 Preliminary Examination Team

*Samples returned from the Apollo 15 site consist of mare basalts and breccias with a variety of pre-mare igneous rocks. The mare basalts are from at least two different lava flows. The bulk chemical compositions and textures of these rocks confirm the previous conclusion that the lunar maria consist of a series of extrusive volcanic rocks that are rich in iron and poor in sodium. The breccias contain abundant clasts of anorthositic fragments along with clasts of basaltic rocks much richer in plagioclase than the mare basalts. These two rock types also occur as common components in soil samples from this site. The rocks and soils from both the front and mare region exhibit a variety of shock characteristics that can best be ascribed to ray material from the craters Aristillus or Autolycus.*

The prime scientific objective leading to the exploration of the moon is the characterization of this body as a planet. In particular, we desire to determine its present chemical and physical structure and to infer from these its initial state. A most important element in planning the exploration of the lunar surface is the choice of sites to be studied. For the most comprehensive coverage of the lunar surface, each landing site should have access to terrain with a variety of structural, temporal, and chemical characteristics. The Apollo 15 landing site is set between mountains that rise more than 4000 m above it and valleys that cut more than 300 m into the surface.

Hence, samples from this region cover a wide range of stratigraphic units and provide an insight into the subsurface structure of the moon. The morphology, mineralogy, petrology, and chemistry of the Apollo 15 samples are described in this article. In addition, several preliminary hypotheses relating individual samples to a geological framework are suggested. An accompanying report (1) describes the selenological significance of the samples.

It should be mentioned, however, that the samples represent three distinct selenological units or structures: (i) the Apennine Front, a major mountain range that was produced during a collision of the moon with

an asteroid-sized object, (ii) a series of horizontal lava flows that fill a part of the impact-produced basin, and (iii) a ray of ejecta from a large, young crater that postdates the filling of the basin. The preliminary observations reported here further characterize each of these major units. For example, several distinct types of igneous rock can be associated with different flows that fill the mare basin. The Apennine Front samples are readily distinguished from the samples collected at the Fra Mauro site. They suggest that there are at least two major rock types within the Apennine Front at this locality. The preliminary descriptions do not clearly differentiate Imbrium ejecta from possible pre-Imbrium materials within the mountain front. Neither do they identify material that originated at a great depth, 20 to 30 km, within the moon. The resolution of these questions must await a more detailed study of the Apollo 15 samples.

More than 350 individual samples, weighing altogether 77 kg, were collected from ten sampling areas in the Hadley region during three lunar surface excursions on 31 July and 1 and 2 August 1971. These consist of individual rock specimens ranging in weight from 1 or 2 g to more than 9.5 kg, core tubes, and a variety of soil specimens. The samples come from two distinct selenologic regions, the mare plain and the foot of a mountain, 3000 m high, known as Hadley Delta. The rocks from the mare plain consist of two basic types, (i) extrusive and hypabyssal basaltic rocks and (ii) glass-coated and glass-cemented breccias that are apparently concentrated in the region around the lunar module (LM) [see figure 6 in (1)]. The rock samples from the foot of the front constitute a very diverse set of rock types that range from breccias to possible metaigneous rocks. Thirteen soil samples with an aggregate weight of 4.5 kg were collected from the mare plain, and 18 soil samples with an aggregate weight of 8.5 kg were collected from the mountain front.

Small rock specimens with average dimensions ranging from 0.5 to 6 cm

The membership of the Preliminary Examination Team is as follows. The steering group are P. W. Gast, W. C. Phinney, M. B. Duke, L. T. Silver (California Institute of Technology, Pasadena), N. J. Hubbard, G. H. Heiken, P. Butler, and D. S. McKay. The mineralogy and petrography group are J. L. Warner, D. A. Morrison, F. Horz, J. Head (Bellcomm, Inc, Washington, D.C.), G. E. Lofgren, W. I. Ridley, A. M. Reid, H. Wilshire (U.S. Geological Survey, Menlo Park, California), J. F. Lindsay (Lunar Science Institute, Houston, Texas), W. D. Carrier, P. Jakes (LSI), M. N. Bass, P. R. Brett, E. D. Jackson (U.S. Geological Survey, Menlo Park, California). The chemical analysis group are J. M. Rhodes (Lockheed Electronics Company, Houston), B. M. Bansal (LEC), J. E. Wainwright (LEC), K. A. Parker (LEC), and K. V. Rodgers (LEC). The gamma-ray counting group are J. E. Keith, R. S. Clark, E. Schonfeld, L. Bennett, M. Robbins (Brown and Root-Northrup, Houston), and W. Portenier (BRN). The noble gas analysis group are D. D. Bogard, W. R. Hart (BRN), W. C. Hirsch (BRN), and R. B. Wilkin (BRN). The carbon analysis group are E. K. Gibson, C. B. Moore (Arizona State University, Tempe), and C. F. Lewis (ASU). Those members listed with no institution are from the NASA Manned Spacecraft Center, Houston.

Table 1. The range of percentages of main particle types in the soil samples (0.125- to 0.25-mm fraction).

Station	Agglutinates and brown glass	Green glass droplets	Basalt	Clino-pyroxene	Feldspar	Micro-breccias*	Samples
LM	71.4		4.0	8.0	1.0	5.5	
8	63-67	3.5-3.0	5-6.5	13	2.5-3.5	2.0	2
6	23-64	3-11.5	3-8.0	9-13	2.5-12	7-32	5
2	45-53	3-8	2.0	8-14	7-13	7-13	4
7	14-42	37-47	2.8-5.5	7.5	3.0	0-9	2
9a	30-36	1-4	16.0	30-35	4-8	5.0	2
9	55	4.5	6.0	20	5.0	5.5	1

\* Vitric and recrystallized.

were collected at three sampling sites, St. George Crater, Spur Crater, and the rille edge. These samples were obtained by raking or sieving the soil in these regions and are statistically representative of the smaller rock fragments found at these sites. They include fragments of several rock types not represented among the larger samples.

A macroscopic study was made of all the rock samples, and more detailed petrographic and chemical studies were made of a smaller set of samples. Most of the individual soil samples were analyzed both in thin section and by microscopic examination of several

hundred grains of each soil. At this stage, studies of the core tubes were limited to nondestructive x-radiographs leading to gross textural characterization.

The samples selected for chemical and isotopic studies and thin section analysis were limited to a representative set chosen for preliminary characterization of the entire Apollo 15 collection by the Preliminary Examination Team and the Lunar Sample Analysis Planning Team (2).

*Mare basalts.* Approximately one-third of the individually collected rock specimens are extremely fresh, basaltic, igneous rocks exhibiting a wide range

of textures that include extraordinary zoned, pyroxene phenocrysts, which penetrate large vesicles or vugs in some samples. These basaltic rocks include massive, dense, fine-grained basalts and slightly vuggy gabbroic rocks, as well as highly vesicular and scoriaceous rocks that consist of more than 50 percent void space. Even a cursory macroscopic textural description indicates that the conditions of crystallization of these rocks varied widely. Several precisely oriented rock chips were removed from large boulders on the lunar surface. Two such chips were taken from a rock that may have been only moderately reoriented since its time of solidification.

The return of such well-documented samples makes possible a variety of experiments that could not be undertaken with the igneous samples returned from previous sites. It may, for example, be possible to infer the orientation of the local lunar magnetic field more than  $3 \times 10^9$  years ago. It should also be possible to determine the age of one of the major secondary craters, Dune Crater, from the samples collected at its rim. The exposures observed at the rille edge, as illustrated in Fig. 1, suggest that the mare basalts collected at this site may come from a series of basalt flows up to 30 m in thickness.

The chemical composition of seven individual basalt samples is given in Table 1. These include representatives from all of the mare sampling points, along with a single metabasalt (15256) collected at station 6 at the foot of the front. The range of compositions observed in these seven analyses is remarkably small, the greatest variation being found in the MgO, FeO, and TiO<sub>2</sub> contents. In the context of other lunar basalts or terrestrial basalts, these rocks are similar to those found at Statio Tranquillitatis and at the Apollo 12 and Luna 16 sites. In particular, the high iron content and correspondingly high FeO/MgO ratio should be noted. Also as in previous mare basalts, the low Na<sub>2</sub>O content distinguishes the lunar samples from all terrestrial basalts. The average TiO<sub>2</sub> content is somewhat lower than that observed at previous mare sites. A more detailed comparison of the Apollo 15 mare basalts with terrestrial and other lunar samples is given in Figs. 2 and 3. The FeO concentrations (Fig. 2) reveal the systematic difference in iron content of mare basalts and terrestrial and lunar highland ba-

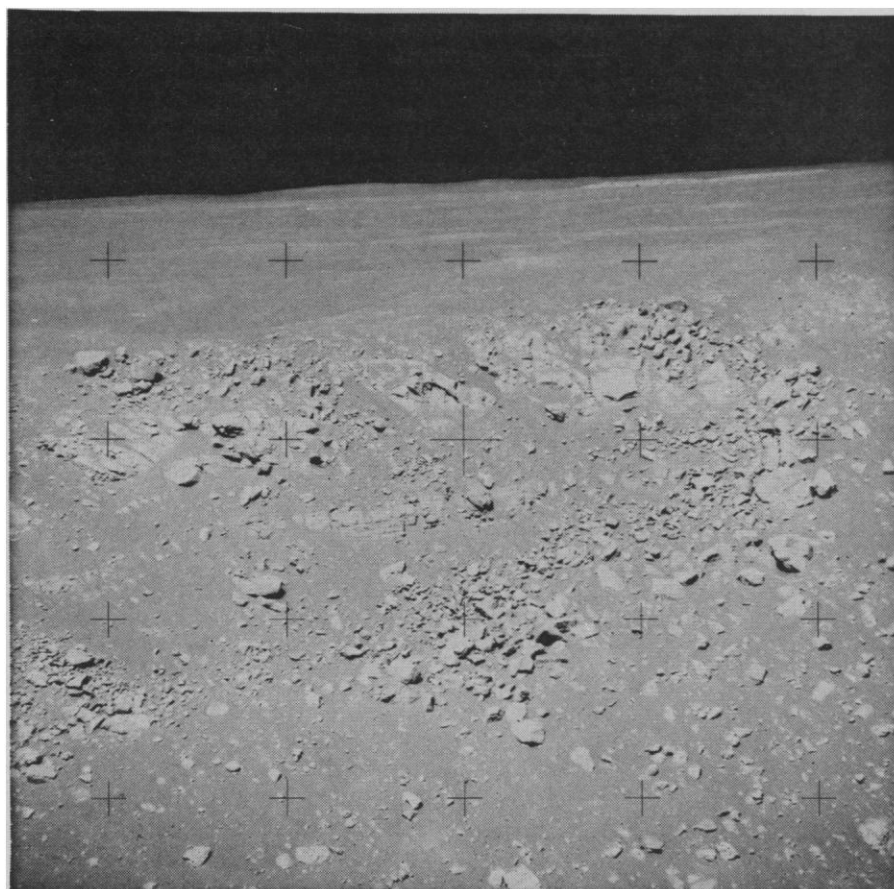


Fig. 1. View of layering in the western wall of Hadley Rille as seen from station 9. The top layer appears to be relatively thick (about 25 m), but the next series of layers are relatively thin. The total width of the far wall in the photograph is 150 m.

Table 2. X-ray fluorescence analyses of igneous and metigneous rocks from the Apollo 15 site. Each major element (except Na) was determined on a 280-mg aliquot of a sample prepared according to the procedure of Norrish and Hutton (9). Sodium was determined by atomic absorption spectrometry; a 20-mg sample was used. Except for Sr and Zr, concentrations are given as percents by weight; ppm, parts per million.

Component	Location and sample number									
	Seat belt station 15016	ALSEP 15058	Elbow Crater 15076	"Meta-basalt" station 6 15256	Dune Crater 15499	Rille station 15555	Rille station 15556	Anorthosite 15415	Gabbroic anorthosite 15418	Apollo 14 control sample 14310
SiO <sub>2</sub>	43.97	47.81	48.80	44.93	47.62	44.24	45.11	44.08	44.97	47.19
TiO <sub>2</sub>	2.31	1.77	1.46	2.54	1.81	2.26	2.76	0.02	0.27	1.24
Al <sub>2</sub> O <sub>3</sub>	8.43	8.87	9.30	8.89	9.27	8.48	9.43	35.49	26.73	20.14
FeO	22.58	19.97	18.62	22.21	20.26	22.47	22.25	0.23	5.37	8.38
MnO	0.33	0.28	0.27	0.29	0.28	0.29	0.29	0.00	0.08	0.11
MgO	11.14	9.01	9.46	9.08	8.94	11.19	7.73	0.09	5.38	7.87
CaO	9.40	10.32	10.82	10.27	10.40	9.45	10.83	19.68	16.10	12.29
Na <sub>2</sub> O	0.21	0.28	0.26	0.28	0.29	0.24	0.26	0.34	0.31	0.63
K <sub>2</sub> O	0.03	0.03	0.03	0.03	0.06	0.03	0.03	< 0.01	0.03	0.49
P <sub>2</sub> O <sub>5</sub>	0.07	0.08	0.03	0.06	0.08	0.06	0.08	0.01	0.03	0.34
S	0.07	0.07	0.03	0.08	0.07	0.05	0.08	0.00	0.03	0.02
Cr <sub>2</sub> O <sub>3</sub>						0.70			0.11	0.18
Sum	98.54	98.49	99.08	98.66	99.08	99.46	98.94	99.95	99.41	98.87
Sr (ppm)	83	101	99	100	105	92	107	184	152	189
Zr (ppm)	95	98	50	90	112	78	91		67	847
<i>Normative composition</i>										
Quartz	0.00	1.15	1.61	0.00	0.38	0.00	0.00	0.10	0.00	0.16
Orthoclase	0.18	0.18	0.18	0.18	0.36	0.18	0.18	0.06	0.18	2.90
Albite	1.78	2.37	2.20	2.37	2.45	2.03	2.20	2.88	2.62	5.25
Anorthite	21.97	22.86	24.12	22.91	23.82	21.97	24.48	95.29	71.46	50.73
Diopside	20.25	23.35	24.56	23.27	22.90	20.51	24.26	1.22	6.73	6.58
Ferrohypersthene	32.14	44.97	43.55	35.76	45.48	32.12	37.53	0.00	12.38	29.93
Olivine	17.61	0.00	0.00	9.14	0.00	17.47	4.70	0.00	5.33	0.00
Ilmenite	4.39	3.36	2.77	4.82	3.44	4.29	5.24	0.04	0.51	2.36

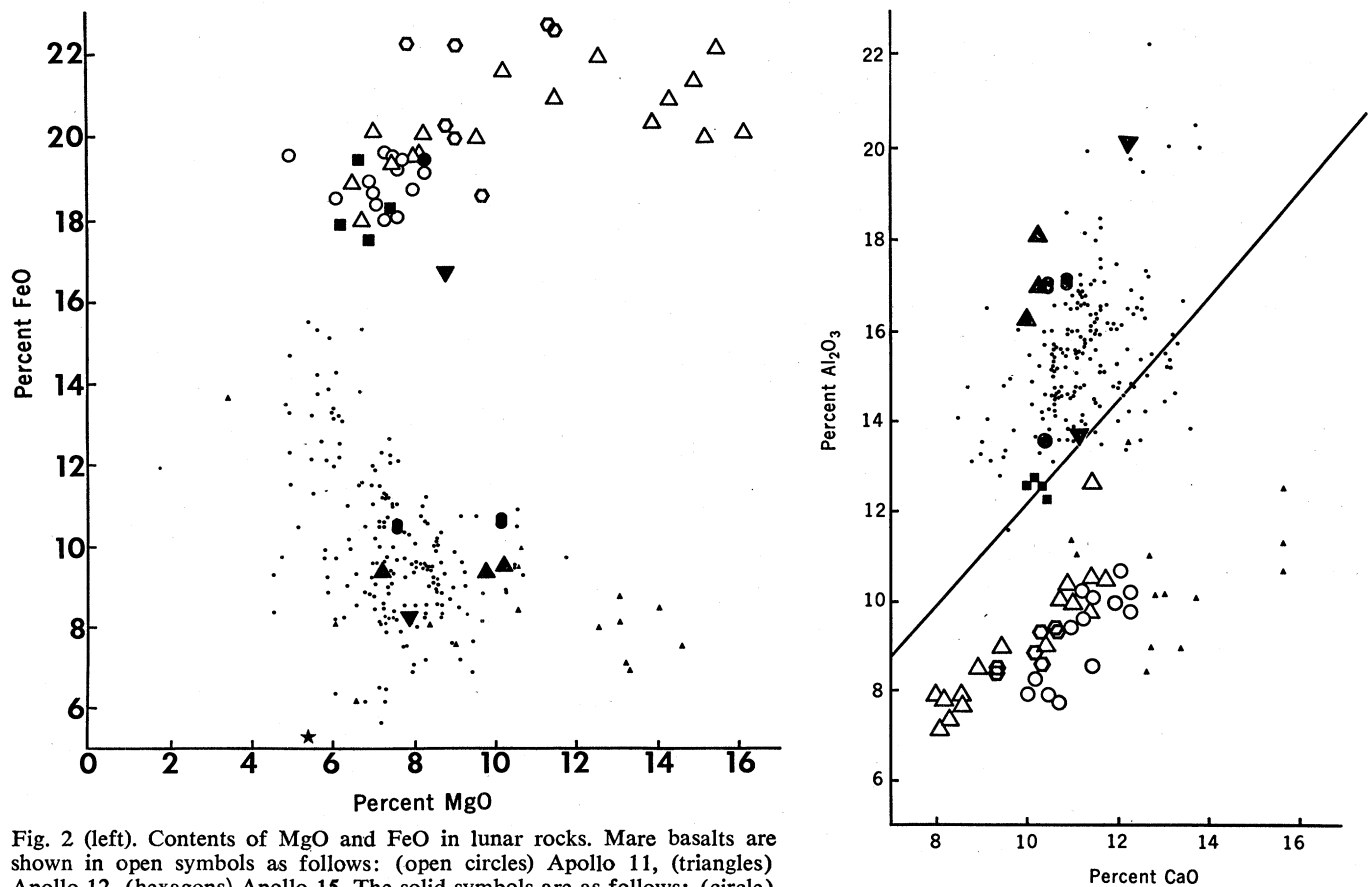


Fig. 2 (left). Contents of MgO and FeO in lunar rocks. Mare basalts are shown in open symbols as follows: (open circles) Apollo 11, (triangles) Apollo 12, (hexagons) Apollo 15. The solid symbols are as follows: (circle) Luna 16, (triangles, apex down) Apollo 14 igneous rocks, (triangles, apex up) three averages of noritic or KREEP (11) fragments from Apollo 12 soil, (oblong circles) two averages of several hundred individual particles from the Apollo 14 soil, (squares) four eucrites. The star represents Apollo 15 sample 15418. The small dots represent analyses for oceanic ridge basalts and Icelandic basalts taken from the literature. The small triangles represent analyses of Hawaiian olivine nephelinites and melillite basalts. Oceanic basalts and Icelandic basalts are among the most iron-rich extrusive basaltic rocks found on the earth. Fig. 3 (right). Contents of CaO and Al<sub>2</sub>O<sub>3</sub> in lunar and terrestrial basaltic rocks. The symbols are identical to those in Fig. 2. The line is the locus of CaO and Al<sub>2</sub>O<sub>3</sub> contents of all chondrites, eucrites, and howardites.

salts. Both the content of iron and magnesium and the FeO/MgO ratio in a large group of mare basalts are similar to those of eucritic meteorites. Also, the FeO/MgO ratio for four different mare regions falls in a rather narrow range between 2.2 and 3.8 if the high-magnesium basalts, probably enriched in olivine, from the Apollo 12 site are excluded.

The CaO and Al<sub>2</sub>O<sub>3</sub> concentrations (Fig. 3) show that the mare and highland basalts are separated by the Al/Ca ratio of chondritic meteorites. Moreover, when all the mare basalts are considered as a group, there appears

to be a significant correlation between their calcium and aluminum contents. Major terrestrial basalt types also fall on either side of the meteoritic Al/Ca ratio. Oceanic ridge basalts and island arc basalts are generally enriched in aluminum relative to calcium, that is, they have Al/Ca ratios greater than the meteoritic ratio. Conversely, nepheline normative basalts tend to be depleted in aluminum relative to calcium. The comparisons in Fig. 3 suggest that both lunar and terrestrial basalts differ from most meteorites, in which the Al/Ca ratio is essentially constant (3). The variable Al/Ca ratios of lunar

samples argue against the origin of achondrites from the lunar surface.

The abundances of trace elements, including the contents of potassium, uranium, and thorium, of the Apollo 15 basaltic rocks are generally similar to those of the Apollo 12 igneous rocks.

Petrographic thin sections - of 13 different Apollo 15 basalt samples have been examined. All the basalts from the mare regions have primary igneous textures and can be grouped to suggest that there are widespread layers underlying the mare region. A single basaltic rock from the front (15256)

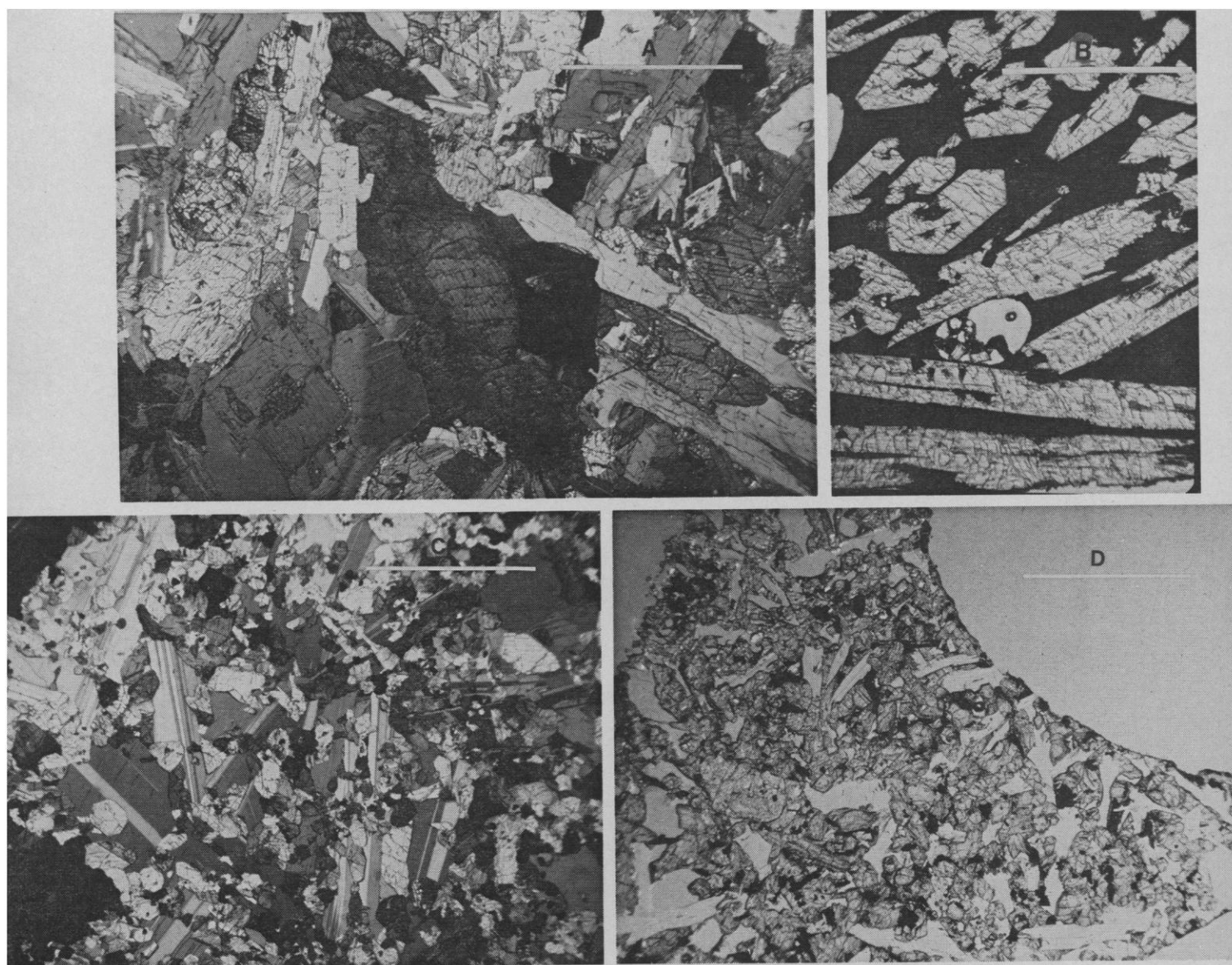


Fig. 4. (A) Sample 15076,12 in thin section (crossed polars), showing zoned clinopyroxene and plagioclase containing cores of pyroxene. The inner zone is pigeonite and the outer zone is augite. The opaque mineral is ilmenite. (Scale bar, 1 mm.) (B) Sample 15485,3 in thin section (plane light), showing skeletal clinopyroxene crystals in a glassy maroon matrix. Note the vesicle containing fragments of crystals and glass. (Scale bar, 1 mm.) (C) Sample 15535,11 in thin section (crossed polars), showing olivine phenocrysts in a ground mass of pyroxene and poikilitic plagioclase. (Scale bar, 1 mm.) (D) Sample 15556,15 in thin section (plane light), showing possible plagioclase phenocrysts in a matrix of granular pyroxene, olivine, and opaques. Note the large vesicles. The scale bar represents 1 mm.

appears to be extensively shock metamorphosed.

Four distinctly different textural types of mare basalts have been recognized in thin section:

1) Porphyritic clinopyroxene basalt (15058, 15076, 15085, and 15475), typified by prisms 3 to 9 mm long with cores of yellow-green pigeonite and rims of brown augite as phenocrysts in a subophitic matrix. The matrix contains moderately to strongly zoned plagioclase with *a*-axial inclusions of pyroxene. Tridymite occurs in these sections (see Fig. 4A).

2) Porphyritic clinopyroxene basalt vitrophyre (15485, 15499, and 15597), typified by skeletal prisms 1 to 7 mm long with hollow cores surrounded by pigeonite and thin rims of augite as phenocrysts in a glassy to devitrified matrix consisting of plagioclase and pyroxene 3  $\mu$ m long in plumose intergrowths. The phenocrysts show preferred orientations. One specimen has a prism of skeletal olivine in addition to pyroxene (see Fig. 4B).

3) Porphyritic olivine basalt (15535, 15545, and 15555), typified by about 10 percent euhedral olivine phenocrysts in an inequigranular matrix of poikilitic plagioclase and a wide range of sizes of weakly zoned clinopyroxene (pigeonite cores to augite rims). Cristobalite occurs in all three thin sections (see Fig. 4C).

4) Highly vesicular (scoriaceous) basalt (15016 and 15556), typified by over 50 percent weakly zoned clinopyroxene (pigeonite cores to augite rims) as part of a subophitic to intergranular texture. Plagioclase is weakly to strongly zoned (see Fig. 4D).

The first type is quite ubiquitous. It is identified in thin sections of samples from Elbow Crater, Dune Crater, and the LM landing site. A macroscopic examination of samples from the rille station (9a) suggests that the same rock type also occurs there. The most detailed collection of this rock type was obtained at three sampling points on a radial traverse 100 m long across the rim of Elbow Crater. The type 1 basalts cover a wide range of grain sizes, from gabbroic at the rim of Elbow Crater (15065), to porphyritic rocks of much finer grain at the rille station. It is tentatively suggested that this variation reflects the ejection of samples from different depths of a thick, widespread unit near the top of the underlying bedrock in this area. A very fine grained, white crust, 0.1 mm thick, occurs along

Table 3. X-ray fluorescence analyses of Apollo 15 soil and breccia samples. Trace elements were determined on a 1-g powder by the procedure of Norrish and Chappell (10). Concentrations are given as percentages by weight or as parts per million (ppm).

Component	Location and sample number												
	Soils					Breccias							
	Apollo 11 soil 10084	Apollo 12 soil 12070	Apollo 14 soil 14163	LM contingency 15021	St. George comprehensive 15101	Front station 6 15271	Spur Crater comprehensive 15301	Dune Crater 15471	Scarplet Crater 15501	Rille comprehensive 15601	Breccia station 6 15265	Rille breccia 15558	Green clod 15923
SiO <sub>2</sub> (%)	41.86	45.91	47.17	46.56	45.95	46.70	45.91	46.10	46.21	45.05	46.94	46.31	45.18
TiO <sub>2</sub> (%)	7.56	2.81	1.79	1.75	1.27	1.47	1.17	1.58	1.81	1.98	1.40	1.89	1.14
Al <sub>2</sub> O <sub>3</sub> (%)	13.55	12.50	17.22	13.73	17.38	16.51	14.53	12.91	12.20	10.20	16.71	12.40	15.06
FeO (%)	15.94	16.40	10.35	15.21	11.65	12.15	14.05	16.24	16.72	19.79	11.18	16.54	13.72
MnO (%)	0.21	0.22	0.14	0.20	0.16	0.16	0.19	0.21	0.22	0.26	0.15	0.22	0.18
MgO (%)	7.82	10.00	9.37	10.37	10.36	10.55	12.12	11.11	10.80	10.89	9.95	10.51	12.14
CaO (%)	12.08	10.43	10.95	10.54	11.52	11.29	10.70	10.42	10.25	9.87	11.19	10.18	11.11
Na <sub>2</sub> O (%)	0.40	0.41	0.66	0.41	0.39	0.43	0.35	0.32	0.37	0.29	0.51	0.42	0.36
K <sub>2</sub> O (%)	0.13	0.25	0.58	0.20	0.17	0.21	0.16	0.12	0.16	0.10	0.25	0.19	0.11
P <sub>2</sub> O <sub>5</sub> (%)	0.11	0.27	0.46	0.18	0.13	0.21	0.15	0.12	0.17	0.11	0.25	0.21	0.09
S (%)	0.15	0.08	0.08	0.06	0.06	0.08	0.04	0.07	0.07	0.06	0.08	0.09	0.06
Cr <sub>2</sub> O <sub>3</sub> (%)	0.32	0.43	0.22	0.06	0.06	0.38	0.04	0.47	0.49	0.56	0.33	0.51	0.40
Sum	100.13	99.71	98.99	99.21	99.04	100.14	99.37	99.67	99.47	99.18	98.94	99.47	99.55
Sr (ppm)	169	136	186	135	142	144	113	124	122	109	150	123	111
Zr (ppm)	312	529	978	410	313	382	260	229	317	199	469	356	152
Nb (ppm)	19	33	65	24	19	23	17	15	20	13	29	22	10
Rb (ppm)	3.3	6.9	15	6.1	4.9	5.6	3.8	3.0	4.7	3.1	7.8	5.3	2.7
Th (ppm)	2.2	6.7	13	3.8	3.3	4.4	4.2	3.0	3.1	<2	4.8	3.6	<2
Ni (ppm)	238	276	322	288	260	268	268	54	72	47	100	78	39
Y (ppm)	105	110	213	91	69	84	60	54	72	47	100	78	39

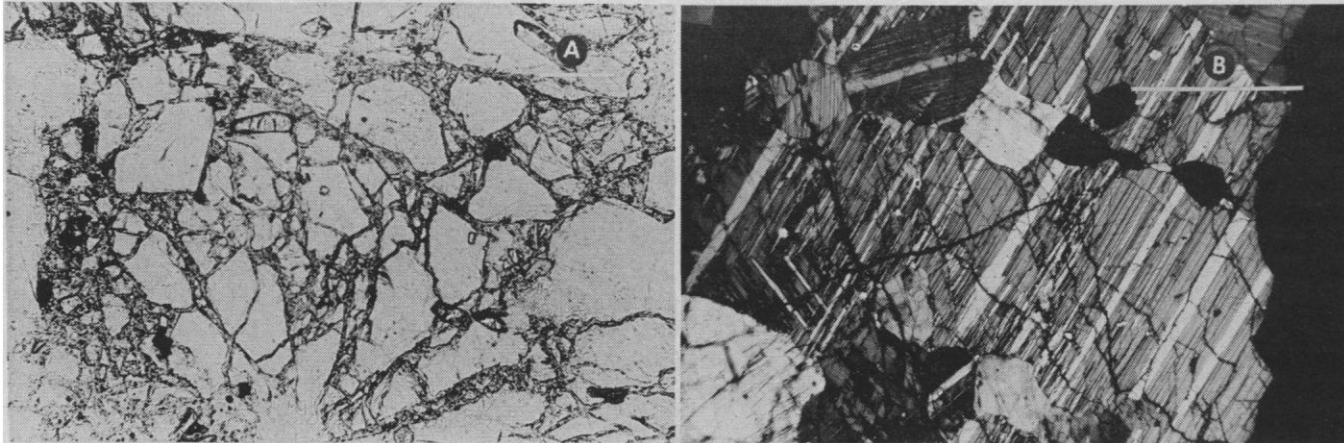


Fig. 5. Thin sections of anorthosite (15415). (A) Shattered plagioclase fragments surrounded by glass; the scale bar indicates 0.1 mm. (B) Parallel trains of polygonal plagioclase grains that have recrystallized along old fractures in a large plagioclase grain, as evidenced by displayed twin lamellae; the scale bar indicates 1 mm.

fractures of this rock at Dune Crater. These are the first lunar samples with evidence of deposits or alteration that may involve vapor or fluid phases in their formation.

The second type of mare basalt occurs in fragments obtained at the rille and as a large boulder at Dune Crater, from which two identical chips were taken 1 m apart. These sites occur at the extremities of the region that was sampled, which suggests that this basalt type may also be a widespread unit in the underlying bedrock.

Most of the samples of the third and fourth types of mare basalts come

from the station at the edge of the rille. A single sample of type 3 was found halfway between Elbow Crater and the LM. In addition, some fragments of the type 3 basalt may occur in the rake sample taken at Spur Crater. At this stage, the distribution of samples of these two basalt types does not lead to any clear-cut hypotheses that relate them to the underlying bedrock.

*Nonmare basalts.* Samples from the previous Apollo missions provide rather strong evidence that the premare lunar surface contained basaltic rocks richer in plagioclase and poorer in

ferromagnesium and opaque minerals than the mare basalts. One of the objectives of the Apollo 15 mission was to elucidate the occurrence of these nonmare materials on the lunar surface. It was anticipated that such samples could occur at the Apennine Front, either as deep-seated ejecta brought to this region by the Imbrium collision or as subsurface materials brought to the surface by the faulting responsible for the Apennine Front. In either case, the samples in this region should have a much more complicated history than the mare basalts and thus be much more difficult to

Table 4. Gamma-ray analyses of Apollo 15 samples. Only the last three digits of each sample number are given here; ppm, parts per million; dpm, disintegrations per minute.

Sample or section number	Weight (g)	Depth (cm)	K (% weight)	Th (ppm)	U (ppm)	K/U	<sup>26</sup> Al (dpm/kg)	<sup>22</sup> Na (dpm/kg)	β <sup>+</sup> (dpm/kg)
<i>Soils (&lt; 1 mm)</i>									
431	145.4		0.19 ± 0.02	4.8 ± 0.7	1.1 ± 0.2	1730	68 ± 14	36 ± 5	
021	132		0.16 ± 0.02	5.1 ± 0.7	1.3 ± 0.2	1230	175 ± 25	50 ± 7	
271,16	527.9		0.16 ± 0.03	4.2 ± 0.8	1.2 ± 0.2	1330	130 ± 20	34 ± 5	
211,2	104.2		0.15 ± 0.03	3.8 ± 0.8	0.96 ± 0.20	1530	130 ± 20	57 ± 9	
301	557.2		0.12 ± 0.02	3.2 ± 0.5	0.88 ± 0.15	1360	104 ± 20	40 ± 10	
<i>Breccias and metaigneous rocks</i>									
206	92.0		0.45 ± 0.06	11 ± 2	3.0 ± 0.6	1500	38 ± 15	45 ± 10	
265	314.2		0.19 ± 0.03	5.1 ± 1.0	1.3 ± 0.2	1460	79 ± 15	38 ± 9	
558	1333.3		0.17 ± 0.02	3.4 ± 0.4	1.0 ± 0.1	1700	84 ± 15	36 ± 10	
466	118.0		0.15 ± 0.03	3.5 ± 0.7	0.93 ± 0.20	1610	84 ± 15	40 ± 9	
086	172.1		0.14 ± 0.03	3.2 ± 0.5	0.76 ± 0.11	1840	39 ± 15	40 ± 15	
455	881.1		0.090 ± 0.020	1.9 ± 0.4	0.50 ± 0.10	1800	65 ± 20	39 ± 15	
426,1	125.7		0.082 ± 0.01	1.9 ± 0.4	0.43 ± 0.10	1900	59 ± 12	38 ± 8	
418	1140.7		0.0086 ± 0.0010	0.13 ± 0.04	0.04 ± 0.01	2150	120 ± 40	25 ± 10	
<i>Crystalline rocks</i>									
085	471.3		0.041 ± 0.005	0.51 ± 0.10	0.13 ± 0.03	3150	71 ± 15	33 ± 10	
256	201.0		0.034 ± 0.004	0.46 ± 0.10	0.15 ± 0.02	2260	95 ± 15	36 ± 8	
415	269.4		0.012 ± 0.002	0.007 ± 0.030	0.0024 ± 0.007		115 ± 15	36 ± 5	
<i>Drill stems</i>									
6-3		11-21	0.19 ± 0.03	4.7 ± 1.0	1.3 ± 0.3	1460	57 ± 20	33 ± 18	77 ± 15
4-2		106-117	0.17 ± 0.03	4.3 ± 1.0	1.1 ± 0.3	1550	16 ± 18	34 ± 15	45 ± 10
1-2		234-245	0.19 ± 0.03	3.7 ± 1.0	1.1 ± 0.3	1730	< 11	< 10	< 9

characterize. A preliminary examination of samples collected from the mountain front provides strong evidence for the existence of a type of basaltic rock that is not found in the mare regions. Fragments of this type of basalt occur both in the rake sample from Spur Crater and as clasts in breccia samples from the front. They are characterized by large proportions of plagioclase relative to ferromagnesian minerals, by the color and homogeneity of the pyroxenes, and by the character and abundance of the opaque minerals. Moreover, the non-mare basaltic rocks are consistently free of vugs and vesicles. An examination of thin sections of several breccia clasts indicates that they are similar to the plagioclase-rich basalt (14310) returned from the Apollo 14 site (4).

*Clastic and metamorphosed rocks.* A wide assortment of rocks whose textural characteristics indicate multiple events in their origins have been returned from the Apollo 15 site. Although the greatest variety of these rocks was concentrated along the foot of Hadley Delta, breccias of various types were found throughout the entire area. The front collection contains a number of unique specimens that cannot be more generally characterized. Several individual specimens that deserve particular mention are discussed in detail below.

Much of the material collected at the front is ultimately derived from basic igneous rocks, that is, extrusive basalts or cumulates enriched in plagioclase. Unlike the mare samples, however, all of the front samples have undergone substantial shock metamorphism or brecciation followed by lithification in the interval between the crystallization of the igneous source rock and the time of deposition of the rocks at their present site. It is not yet clear whether most of the shock metamorphism and brecciation was post-Imbrium, that is, followed the formation of the mountain front, or whether some of the breccias existed in essentially their present form prior to the Imbrium impact. In other words, it is not known whether any of the igneous rocks contained in the breccias are derived from igneous structures that underlie the debris layer now covering the mountain front where these samples were collected.

One fragment of extremely pure anorthosite (15415) was recognized as an anorthosite during the lunar surface



Fig. 6. Thin section of 15418,8 (plane light). The outer zone is of swirled, devitrified glass, and the two inner zones are of intergrown plagioclase needles (light gray) and pyroxene (dark gray). Note the vesicles throughout the section. The scale bar represents 1 mm.

traverse. Photographs from the lunar surface show that this rock was perched on a pedestal of breccia, which suggests that the anorthosite was a clast in a breccia. The bulk chemical composition and normative compositions are given in Table 2. Studies of this sample in thin section reveal that the rock is composed of over 99 percent plagioclase grains (95 to 98 percent anorthite) 1 to 3 cm across, and approximately 1 percent clinopyroxene, 0.1 mm across, consisting of interstitial augite and pigeonite, and augite inclu-

sions in large plagioclase crystals. The wide range of crystal dimensions in this rock makes it difficult to describe its texture with a single photomicrograph. Furthermore, thin sections of the rock reveal a variety of cataclastic textures, including at least two distinct types of postcrystallization deformation. Small patches of highly fractured and shattered plagioclase surrounded by glass are observed in one or two sections (Fig. 5A). They suggest that this anorthosite fragment was involved in a substantial impact subsequent to its crystallization. In addition, polygonal plagioclase grains 0.1 to 1.3 mm in average dimension often occur along fractures within a single crystal of plagioclase (Fig. 5B). Similar polygonal grains also occur along the crystal boundaries. These grains suggest that an older deformation and annealing took place during either the original cooling of the anorthosite or a subsequent period of high temperature.

A thin section of the material in which the fragment of anorthosite was

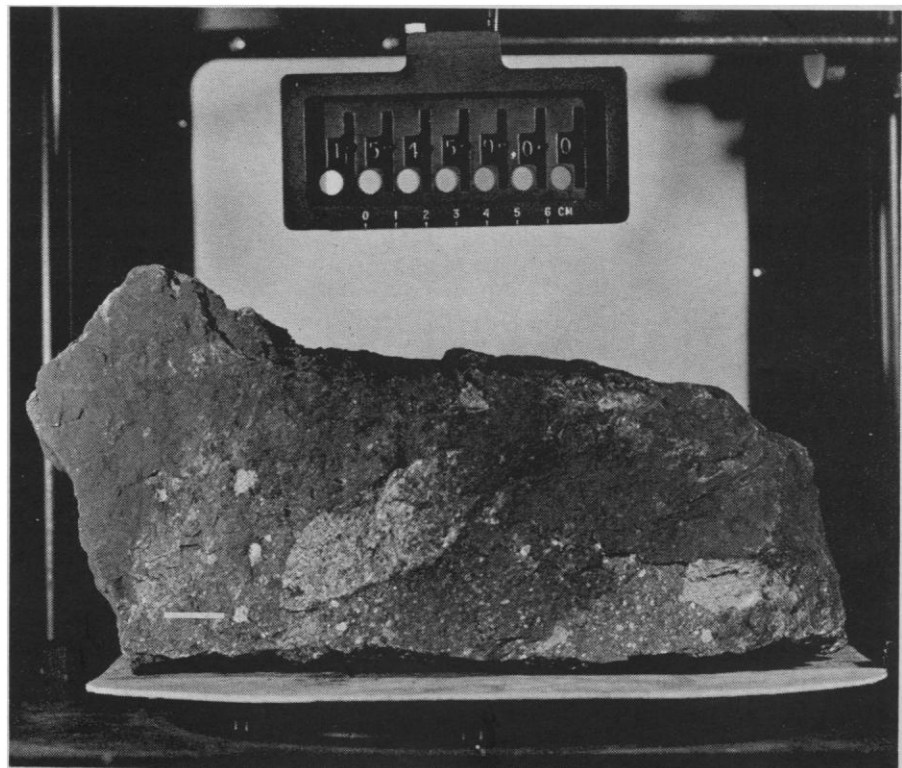


Fig. 7. Coarse breccia (15459) from the rim of Spur Crater. The largest visible clast is 8 cm across. The glassy matrix makes up over 50 percent of the breccia.

Table 5. Characteristics of cores collected.

Location	Length (cm)	Mass (g)	Number of textural layers	Bulk density (g/cm <sup>3</sup> )
Station 2, along the outer edge of a crater 10 m in diameter	63.9	1279	14	1.36 ± 0.05 to 1.66 ± 0.02
Station 6, inside the rim of a subdued crater	36.2	622	4	1.35
Station 9a, at the edge of Hadley Rille	65.5	1401	9	

probably included reveals a complex set of flow-banded glass, glassy breccia, anorthosite fragments, and basaltic material. These textural characteristics give further evidence of the eventful history of this unique rock.

A second unique rock (15455) consists of one-half white material and one-half black material, with inclusions of white in black along the contact area. Thin-section study indicates that the white portion is a severely shattered norite with about 75 percent plagioclase and 25 percent orthopyroxene. A reconstruction of the relict grains indicates coarse plagioclase grains with interstitial orthopyroxene. The black material, which occurs as black veins in the norite, is a breccia containing clasts of norite, anorthosite, and nonmare basalts.

Two rocks (15256 and 15418) appear to be igneous rocks melted by shock. Rock 15256 contains a mixture of clasts, or inclusions, in fine-grained laths of clinopyroxene and plagioclase aligned along a curving structure of the flow type. Its chemical composition (Table 2) is nearly identical to that of the mare basalts high in iron. It seems likely that this rock was ejected from the mare plain onto the front by a collision of sufficient magnitude to metamorphose a dense, crystalline rock. Rock 15418 is unique in texture and in its chemical composition, which is that of a gabbroic anorthosite (Table 2) very rich in anorthite. The FeO/MgO ratio (Fig. 2) of this rock indicates that it was not derived from liquids with the high ratio of the mare basalts. In fact, we suggest that its FeO/MgO ratio relates this plagioclase-rich rock to the basalt type with high aluminum and low iron contents found at the Apollo 14 site and in the Apollo 12 soil fragments.

The thin sections of this rock reveal a banded structure of devitrified glass and microcrystalline basalts (Fig. 6), as well as patches of devitrified maskelynite, annealed pyroxene, and micro-

crystalline basalt. This structure suggests that the fragment was completely melted by shock and subsequently crystallized or annealed. The potassium content of this rock was determined by gamma-ray counting as less than 100 parts per million, which is lower than that of any extrusive basalt found on the lunar surface and suggests that the source of the rock was an igneous cumulate. Moreover, the low potassium content implies that there was very little admixture of soil or regolith during the impact event that produced the rock.

The largest sample returned from the front was a coarse breccia (15459) with clasts up to 8 cm across (see Fig. 7). This sample was collected at the rim of Spur Crater. It is a tough, dense breccia with a matrix having a substantial proportion of glass. The most abundant clasts consist of light-colored basalt and anorthosite, but a

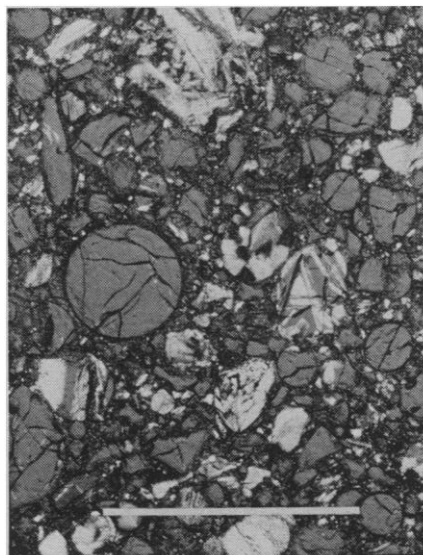


Fig. 8. Thin section of green rock (15426); green glass spheres of various sizes and fragments of green glass (medium gray areas) are shown. The large bright areas are devitrified green glass spheres with small patches of nondevitrified green glass remaining (see center of photograph). The scale bar indicates 0.5 mm.

few basalt clasts similar to mare basalts are also observed. The overall clast characteristics indicate that this breccia sample is probably derived from a nonmare terrain in which a small amount of mare material is present.

The largest rock closely observed at the front was seen at station 2 on the flank of St. George Crater. Two oriented samples (15205 and 15206) from this 1- to 2-m block were returned. Both the surface photographs and the two samples indicate that this rock is a typical breccia. It consists of a matrix with large amounts of devitrified glass in which are set clasts of nonmare basalt and gabbro. The potassium, uranium, and thorium contents of 15206 are higher than those of any other samples studied in this preliminary examination. They approach those of the Apollo 14 breccia samples (4).

During the surface traverse, an unusual green material was noticed at the rim of Spur Crater. Several friable fragments of this sample (15426) were returned. Microscopic studies of these fragments reveal that they are breccias consisting of more than 50 percent green glass occurring as spheres and fragments of spheres (Fig. 8). Many of the green glass spheres have partially devitrified to crystals of orthopyroxene. In a few cases, these crystals occur in a radiating pattern similar to that seen in many meteoritic chondrules. Chemical analyses of both this material (15426) and associated soil samples (15301) show an unusually high MgO concentration. Similar green glass spheres are abundant in the samples of Spur Crater soil and are present in smaller amounts in most other soil samples.

The breccias collected from the mare plain are clearly distinguished from the front breccias by the high abundance of mare basalts and opaque minerals in the former and the high abundance of nonmare basalts and gabbroic rocks and low abundance of opaques in the latter.

The breccias from both the front and the mare region contain unde- vitrified glass either in the matrix or as clasts. Of the 15 thin sections of breccias, 13 have a significant amount of brown glass as matrix, some as much as 50 percent of the rock. Of the remaining two thin sections, one contains partly devitrified glass in the matrix but clear glass clasts. The other (15405) is the only section with a

clearly recrystallized, or annealed, matrix, but, even in this case, there are undevitrified clasts of clear glass. The lack of recrystallized glass in the breccia matrix clearly distinguishes the Apollo 15 breccias from the Apollo 14 breccias, in which recrystallization of glass was common.

Although essentially all the breccias are unrecrystallized, many show a complex history of events. In several cases, where glass veinlets crosscut other breccia components and transect the preferred orientation, remobilization of the matrix material is indicated. In other cases, faulting of glass spheres and other clasts indicates a mechanical disruption of previously existing breccia. Apparently, multiple stages of melting and fracturing can occur without any evidence of recrystallization.

The diverse textural characteristics of the breccias can be grouped into (i) the characteristics of the clasts, which vary from primary igneous rocks to polymict breccias and (ii) the character of the matrix, which varies in both the proportion of glass and the degree to which the matrix is recrystallized. Viewed as a group, the Apollo 15 breccias differ from the Apollo 14 breccias in both of these categories. The Apollo 15 clasts are in large proportion made up of primary igneous rocks, in contrast to the Apollo 14 clasts, which consist of preexisting breccias. The matrix of the Apollo 15 breccias is distinct from that of the Apollo 14 breccias in the striking abundance of unrecrystallized glass. The characteristics of the Apollo 15 breccias, unlike those of the Apollo 14 breccias, cannot all be readily ascribed to the Imbrium collision. How many of these breccias were produced by Imbrium or even by pre-Imbrium events must be considered in the detailed study of these samples.

*Soil samples.* The 31 different soil samples returned from this mission represent at least three distinct regions, that is, the mountain slope, the mare, and the ray or ridge that trends about 30° west of north through the landing site. Four large soil samples, weighing about 1 kg each, were returned for a detailed characterization of these regions. A 100-mg portion from each of 18 of the soil samples was examined microscopically to characterize the different soil types. The distribution of particle sizes was determined by sieving and by direct measurement of the individual grains with a com-

puter-controlled optical measuring system. The grain size distributions for a number of soil samples are summarized in Fig. 9.

The particle types in the Apollo 15 soils are similar to those in the soils from the previous missions in most respects. The major difference is the presence of green glass spheres with an index of refraction of 1.65. The green glasses are different from any glass component previously observed in lunar soils. They are remarkably homogeneous and nonvesicular and are identical to the green glass found in sample 15426. Other glasses, mainly brown and gray, occur as both droplets and angular fragments. With the exception of the green glasses, which are clear, most of the glasses contain detrital and crystal inclusions and may also exhibit a variety of devitrification textures. A summary of the particle types and their relative proportions in different soil samples is given in Table 1.

The soils from stations 2 and 7 are probably most representative of the

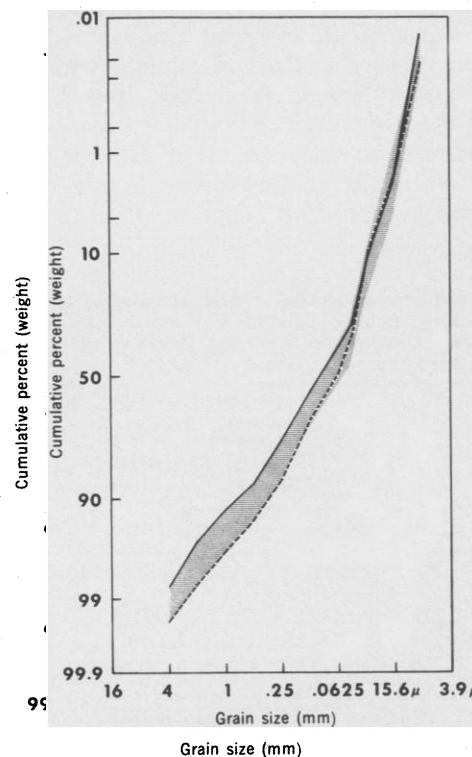


Fig. 9. Grain size distributions for representative soil samples from stations 2, 6, 7, 8, 9, and 9a and the LM site plotted on a probability scale. Most of the curves are very similar, and the range is plotted here as a shaded band. The solid line represents the coarsest grained soil from station 9a, and the dashed line represents soil from station 8. Median grain sizes range from 42 to 98  $\mu\text{m}$ . All soil samples are poorly sorted. Most of the soils are slightly finer grained than soils from other landing sites.

Apennine Front. The station 7 soils, collected close to station 6, are from the edge of the relatively fresh Spur Crater, 100 m in diameter, which may have penetrated any surficial ray material to excavate debris from the Apennine Front. The soils appear to have been derived from several types of microbreccia, granular basalts, and clastic rocks composed of green glass, all of which could be rock types derived from the stratified rocks visible on the upper slopes of Hadley Delta. The variable abundance of the unique green glass component and its concentration in soil and breccia samples from Spur Crater indicate that it may be an important tracer in the study of the regolith at this site.

The sites in the vicinity of the LM are located on a narrow ridge that trends south-southeast to the South Cluster of secondary craters. If the trend of the ridge were continued, it would intercept station 6. Except for differences in the content of green glass, the soils from station 6 are very similar to the soils from the LM area. This ridge has been interpreted by Carr and El Baz (5) as a ray from Aristillus or Autolycus. The similarity of the soil samples collected along this trend may be further evidence for the presence of this ray.

The rille soils are what one would expect from comminuted basalt flows. The microbreccia component may have been derived from the debris extending out from the Apennine Mountains or from the well-stratified rocks interbedded with basalt flows in the rille wall. The soil collected at station 9 is a hybrid of the soils from the LM area and the rille edge.

*Soil chemistry.* The chemical compositions of seven soil samples are given in Tables 3 and 4. These compositions are systematically different from the compositions of the rocks that presumably underlie the soil samples, particularly in the mare regions. In these regions, as at other mare sites, the soil has a much higher  $\text{Al}_2\text{O}_3$  content and much lower FeO content than the associated igneous rocks. Furthermore, the Nb, K, U, and Th contents of all the soils are systematically greater than those determined for the igneous rock 15555. In addition, individual soil samples from the mare region differ in composition from each other, particularly in the characteristics that distinguish the soil from the mare basalts.

The rille soil is in all respects more

like the mare basalts than the soil collected in the vicinity of the LM. The three soil samples from the front are consistently higher in  $\text{Al}_2\text{O}_3$  and lower in FeO than the mare soils. However, the concentrations of other elements, such as K, Y, and Nb, do not distinguish front soil from mare soil. The higher  $\text{Al}_2\text{O}_3$  and lower FeO contents of the front soil again suggest that aluminum-rich units must occur in abundance in the mountain front from which this soil was at least partially derived. Figure 10 illustrates the inverse correlation of FeO and  $\text{Al}_2\text{O}_3$  concentrations for the soil and breccia samples from this site. This correlation is nearly linear between 20 and 8 percent  $\text{Al}_2\text{O}_3$  and 22 and 10 percent FeO. It is significant that the points for samples 15415 and 15418 do not fall on the line drawn for the soil and breccia samples. However, the point for Apollo 14 sample 14310 does fall on the soil and breccia line. Thus, the clasts in the front breccia and the average composition of the front soil suggest that the dominant material found in the mountain front may be a basalt rich in plagioclase. In other words, the two end members responsible for the linear correlation seen in Fig. 10 may be an iron-rich mare basalt and an aluminum-rich, iron-poor premare basalt.

**Cores.** A substantial portion of the soil returned from the Apollo 15 land-

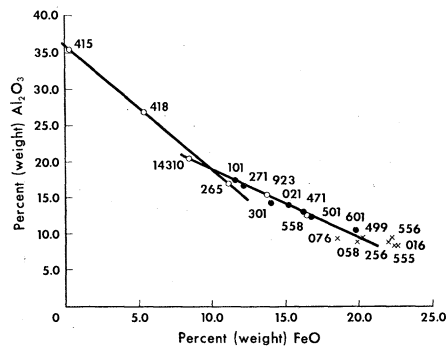


Fig. 10. The contents of  $\text{Al}_2\text{O}_3$  and FeO for Apollo 15 soil and rock samples. (Crosses) igneous rocks, (solid circles) soil samples, (open circles) breccias and aluminum-rich igneous rocks.

ing site was in the form of cores of the regolith. A rotary percussive drill, used for the first time on this mission, was employed to obtain a core from the surface to a depth of 2.4 m. The length of this core may be a significant fraction of the regolith thickness at this site. Moreover, the unique location of this sample, in a region where both detritus from the degradation of the mountain front and the Autolycus or Aristillus ray material make substantial contributions to the regolith, makes it particularly useful in an investigation of the transport of soil by local cratering and the extent to which soils are mixed or homogenized because of turnover by secondary impacts. This is

probably the most useful single sample returned from the moon.

The deep drill consists of six sections, each approximately 40 cm long. All except the lower section were returned completely full. The total mass of this core is 1.33 kg. Both the ease of drilling and the density variations found in different sections of the core tube suggest that the upper portion of the regolith may contain layers of different densities. The sample from the lowest section of the deep drill has an unusually high density,  $2.15 \text{ g/cm}^3$ . This is the highest density for any soil sample returned from the lunar surface.

Only nondestructive examinations of the deep core by x-radiograph and gamma-ray counting have been undertaken to date. Stereo x-radiographs of the entire length of the core reveal significant variations in the abundance of small pebbles and show the density variations. Fifty-eight individual layers, 0.5 to 21 cm thick, have been delineated by these somewhat subjective criteria. Both the layers and the occurrence and orientation of individual rock fragments are illustrated in Fig. 11. Gamma-ray measurements made at three different depths in the core tube show that the  $^{26}\text{Al}$  and  $^{22}\text{Na}$  activity decreases markedly in the lowest sections, as was expected.

Three cores with maximum penetra-

Table 6. Contents of noble gases in Apollo 15 soil and breccia samples. All the abundances are  $\pm 5$  to 10 percent based on multiple standard gas analyses. The uncertainties in the isotopic ratios represent 1 standard deviation of multiple measurements. The abundance blank corrections were typically about 1 percent, and in no case greater than 5 percent. The isotopic ratio blank corrections were significant only for  $^{40}\text{Ar}/^{36}\text{Ar}$  and have been applied. STP, standard temperature and pressure.

Sample	Weight (mg)	Specific volume ( $\times 10^{-6} \text{ cm}^3/\text{g}$ at STP)				Specific volume ( $\times 10^{-9} \text{ cm}^3/\text{g}$ at STP)		$^4\text{He}/^3\text{He}$	$^{20}\text{Ne}/^{22}\text{Ne}$	$^{22}\text{Ne}/^{21}\text{Ne}$	$^{36}\text{Ar}/^{38}\text{Ar}$	$^{40}\text{Ar}/^{38}\text{Ar}$
		$^3\text{He}$	$^4\text{He}$	$^{22}\text{Ne}$	$^{38}\text{Ar}$	$^{84}\text{Kr}$	$^{132}\text{Xe}$					
15301,1 fines	6.14	18.8	45,800	110	233	79.9	16.2	2435	12.60 $\pm 0.02$	28.03 $\pm 0.16$	5.37 $\pm 0.01$	1.78 $\pm 0.01$
15021,4 fines	23.71	30.9	74,600	114	229	87.2	11.7	2419	12.68 $\pm 0.04$	27.91 $\pm 0.06$	5.41 $\pm 0.02$	0.747 $\pm 0.005$
15101,2 fines	23.06	24.3	59,450	103	204	70.2	8.68	2444	12.71 $\pm 0.06$	28.56 $\pm 0.29$	5.42 $\pm 0.01$	1.172 $\pm 0.005$
15601,3 fines	7.62	16.8	35,600	58.3	95.1	44.3	5.51	2123	12.61 $\pm 0.02$	25.42 $\pm 0.14$	5.32 $\pm 0.01$	0.932 $\pm 0.005$
15923,2 glass	25.14	1.17	1,756	7.54	3.94	1.63	0.332	1458	11.65 $\pm 0.02$	10.93 $\pm 0.10$	4.59 $\pm 0.005$	4.40 $\pm 0.04$
15923,2 fines	8.92	2.48	5,970	14.5	5.92	4.39	1.54	2413	12.72 $\pm 0.03$	25.38 $\pm 0.12$	5.08 $\pm 0.20$	2.71 $\pm 0.10$
15265,3 breccia	7.67	13.2	27,200	45.9	105	48.8	4.98	2062	12.57 $\pm 0.01$	24.50 $\pm 0.08$	5.33 $\pm 0.02$	1.87 $\pm 0.01$
15298,3 breccia	8.83	22.1	50,600	89.8	203	125	14.4	2289	12.59 $\pm 0.02$	27.71 $\pm 0.13$	5.36 $\pm 0.01$	1.08 $\pm 0.01$
15498,2 breccia	18.93	5.70	15,670	44.4	88.8	22.4	3.27	2748	12.24 $\pm 0.05$	21.00 $\pm 0.09$	5.30 $\pm 0.02$	1.88 $\pm 0.01$
15558,3 breccia	7.47	23.8	49,150	74.2	135	78.9	13.3	2064	12.50 $\pm 0.02$	24.25 $\pm 0.12$	5.31 $\pm 0.02$	1.89 $\pm 0.01$

tions up to 70 cm were also returned with samples weighing altogether 3.3 kg. The dimensions and characteristics of the individual core samples are summarized in Table 5. At present, none of the cores have been opened for examination. However, x-radiographs have been obtained for all tubes for their entire lengths, and descriptions of textural differences within the cores are based on stereo pairs of these x-radiographs. These descriptions are somewhat subjective, as grain sizes and sorting were estimated by comparison with soils of known grain size. Rock fragments larger than 2 mm can be measured and their shapes described. The layering and the distribution of rock fragments in several individual tubes are shown in Fig. 11. All of the cores exhibit layering in soil textures, grain size, and sorting. It appears that the regolith sampled in these cores is not a homogeneous rubble pile but a complicated sequence of clastic sediments made up of ejecta blankets from nearby and distant craters.

**Gamma-ray activity.** The gamma-ray spectra of 19 samples from the Apollo 15 site have been measured by the low-level counting technique described by O'Kelley *et al.* (6). The principal gamma-ray activity is due to the natural radioactivity of K, U, and Th and the radioactivity of  $^{26}\text{Al}$  and  $^{22}\text{Na}$  induced by cosmic rays.

The results of this survey are summarized in Table 4. The uncertainties shown there are largely due to uncertainties in the geometric corrections for differences in thickness and shape between the samples and the standards. Regions at three different depths in the deep drill tube were counted in a special counter with two NaI(Tl) crystals, each 12.7 cm in diameter, in a lead shield. The results of these measurements demonstrate that the deeper parts of the drill penetrate farther than most cosmic-ray secondaries.

The  $^{26}\text{Al}$  and  $^{22}\text{Na}$  activities listed in Table 4 show that the Apollo 15 soil samples, like previous soil samples, have relatively high  $^{26}\text{Al}$  contents. Only the sample (15431) from underneath the anorthosite is low in  $^{26}\text{Al}$  activity. The breccias and crystalline rocks generally have a somewhat lower  $^{26}\text{Al}$  activity and, on the average, a lower  $^{26}\text{Al}/^{22}\text{Na}$  ratio. Two samples from the Apollo 15 site (15206 and 15086) have  $^{26}\text{Al}/^{22}\text{Na}$  ratios less than 1. In the absence of any evidence for unique chemical compositions for these speci-

mens, it is suggested that they may have been brought to the surface where they were exposed to cosmic rays less than 1 million years ago.

The concentrations of primordial radionuclides ( $^{40}\text{K}$ ,  $^{238}\text{U}$ , and  $^{232}\text{Th}$ ) in the soil and breccia samples reveal no clear-cut distinctions between different groups of samples. The inferred potassium contents range from 0.12 to 0.19 percent with the exception of breccia sample 15206, which is unique in its high potassium content. The K/U ratios for all the soil and breccia samples range from 1230 to 1850. The natural radioactivity of the soil and breccia samples from this site is, thus, quite similar to that of the Apollo 12 soil samples. The two mare basalts analyzed here have relatively low potas-

sium contents and relatively high K/U ratios. As expected from its mineralogy, sample 15415 has an unusually high K/U ratio, which can be ascribed to the inability of quadrivalent uranium to substitute into the plagioclase lattice. With this exception, the range of K/U ratios in the Apollo 15 samples is similar to that observed in samples from previous sites. With these additional observations, there appears to be little doubt that the K/U ratio of the moon ( $1.2 \times 10^3$  to  $4 \times 10^3$ ) is distinct from that of the earth ( $1.0 \times 10^4$  to  $1.2 \times 10^4$ ) (7).

**Noble gases.** The abundances and isotopic compositions of the five noble gases, He, Ne, Ar, Kr, and Xe, were determined by mass spectrometry for five soil and four fragmental rock sam-

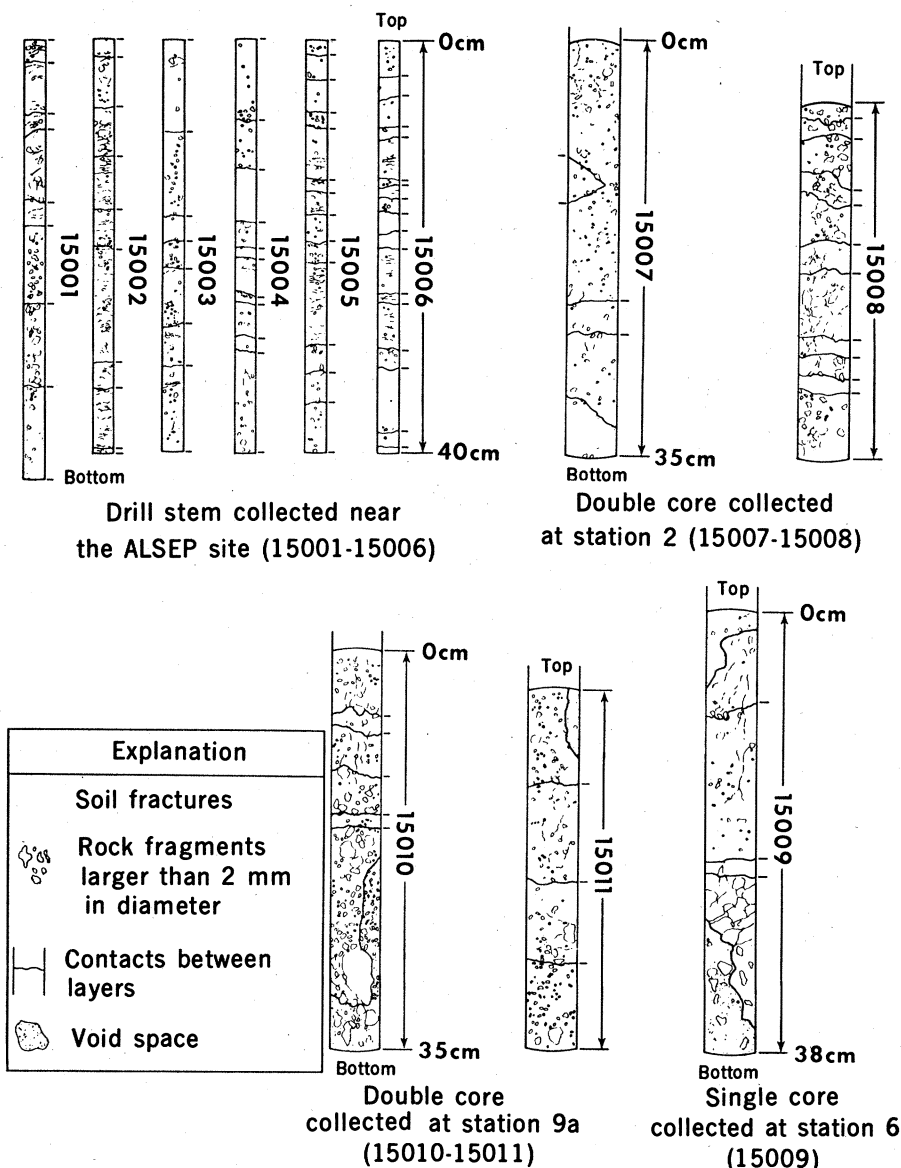


Fig. 11. Sketches of x-radiographs of the six sections of the drill core collected with a rotary percussion drill (samples 15001 to 15006) and of the drive tube cores (samples 15007 to 15011).

ples and are presented in Table 6. Soils 15301, 15021, 15101, and 15601 were sampled over a wide area from locations near the LM, St. George Crater, Spur Crater, and Hadley Rille, respectively. Sample 15923 is soil containing abundant green glass spheres that was collected with rocks 15425 and 15426 near Spur Crater. An almost pure glass fraction and a soil fraction were analyzed separately for this sample. Breccia 15558 was collected near the LM, while the other fragmental rocks were collected near the front.

In most of these Apollo 15 samples, the concentrations of the noble gases are similar to the concentrations determined in Apollo 12 and Apollo 14 bulk soils and somewhat lower than the concentrations in Apollo 11 soils and breccia. These noble gases are predominantly from the solar wind, with smaller amounts of a component produced by nuclear reaction. The elemental abundance ratios fall within the range of values determined previously for lunar soils; the average values (omitting 15923) are  ${}^4\text{He}/{}^{20}\text{Ne} = 45$ ,  ${}^{20}\text{Ne}/{}^{36}\text{Ar} = 6.3$ ,  ${}^{36}\text{Ar}/{}^{132}\text{Xe} = 18,000$ , and  ${}^{84}\text{Kr}/{}^{132}\text{Xe} = 7.5$ . Individual values for the ratios vary by a factor of 2 because of differences in efficiencies for solar wind entrapment and retention. In general, the isotopic composition of the solar wind component is essentially identical to that determined previously for lunar material (4, 7). For the soil samples the trapped  ${}^{20}\text{Ne}/{}^{22}\text{Ne}$  ratio is 12.66, and the trapped  ${}^{36}\text{Ar}/{}^{38}\text{Ar}$  ratio is 5.38.

A number of samples show variations in the  ${}^4\text{He}/{}^3\text{He}$  and  ${}^{40}\text{Ar}/{}^{36}\text{Ar}$  ratios that apparently cannot be explained by differences in radiogenic  ${}^4\text{He}$  and  ${}^{40}\text{Ar}$  contents. Thus, for  ${}^4\text{He}/{}^3\text{He}$ , the value of about 2430 obtained for all the soil samples except 15601 and the value of 2063 obtained for breccias 15265 and 15558 may represent an actual isotopic difference in the trapped solar helium in these samples. Likewise, the trapped  ${}^{40}\text{Ar}/{}^{36}\text{Ar}$  ratios differ by as much as a factor of 3, even after corrections are made for radiogenic  ${}^{40}\text{Ar}$  based on measured potassium contents and an age of  $3.35 \times 10^9$  years. This variation in  ${}^{40}\text{Ar}/{}^{36}\text{Ar}$  exists for those soil samples which possess similar  ${}^{36}\text{Ar}$  contents, and was not noted for Apollo 11 and Apollo 12 soils. Indications are that the variation in this ratio arises from differing contents of  ${}^{40}\text{Ar}$  in the lunar atmosphere. Three out of four breccias have identical  ${}^{40}\text{Ar}/{}^{36}\text{Ar}$  values. It is not

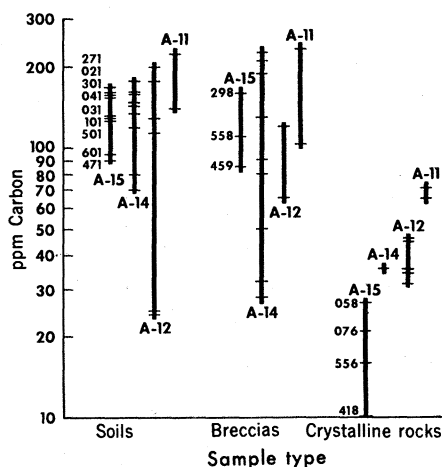


Fig. 12. Comparison of the total carbon abundances for the Apollo 15 sample types with those for the samples from previous Apollo missions (4, 8). Individual samples from Apollo 15 are identified only by their last three sample numbers.

apparent whether the variable  ${}^{40}\text{Ar}$  component in the soils is due to retention efficiencies, geographical distribution of the samples, or some other factor. The low  ${}^{40}\text{Ar}/{}^{36}\text{Ar}$  ratios of all these samples preclude accurate determinations of radiogenic  ${}^{40}\text{Ar}$  from in situ decay of potassium.

The isotopic compositions of Kr and Se in these samples reflect a solar wind origin, with small variable amounts from gases produced by nuclear reactions. The ratios for Kr and Xe in all of these samples are not presented in this article. The isotopic compositions of these elements are essentially identical with those found for soils from other sites, with the exception of small enhancements in the abundance of  ${}^{136}\text{Xe}$ . No evidence was found for excess  ${}^{129}\text{Xe}$  of a radiogenic origin.

The concentrations of  ${}^{21}\text{Ne}$ ,  ${}^{80}\text{Kr}$ , and  ${}^{126}\text{Xe}$  produced by cosmic-ray spallation have been calculated for all of these samples. Differences in exposure ages appear to exist even when variations in target chemistry are considered; the ages fall in the range 50 to 500 million years.

**Total carbon content.** The total carbon contents of 16 samples have been determined by direct combustion of soil or pulverized rock, according to the technique described by Moore *et al.* (8). The results of these analyses are shown in Fig. 12, along with results obtained for Apollo 11, 12, and 14 samples. The carbon content of the soil and breccia samples is systematically higher than that of the Apollo 15 igneous rocks and similar to that of the soil samples from the other Apollo

sites. The carbon content of the Apollo 15 extrusive igneous rocks is significantly lower than that reported for igneous rocks from previous sites. This difference probably results from improved procedures for handling and contamination control.

The shock-melted anorthosite (15418) from the front has an even lower carbon content than the extrusive igneous rocks. This difference can, perhaps, be ascribed to the removal of carbon during shock metamorphism. Alternatively, it may be an indication that the gabbroic anorthosite from which this rock was derived had an even lower carbon content than the extrusive basalts. The low carbon content of this rock further substantiates the earlier assertion that it underwent shock metamorphism with negligible admixture of soil or regolith with the parent rock.

The substantiation of the systematic difference in the carbon content of the soil and igneous rocks appears to confirm the hypothesis (8) that most of the carbon in the lunar soil may be ascribed to the solar wind. We may, thus, infer from the data given here that the carbon content of the moon is much lower than was previously inferred from analyses of the lunar soil or from previous analyses of lunar igneous rocks.

Several specific conclusions can be drawn from this preliminary examination. They are:

- 1) The K/U ratio of both the mare basalts and the soil further establishes the earlier conclusion (7) that the K/U ratio clearly distinguishes the moon from the earth.

- 2) The soil chemistry and the lithology of fragments in the rake sample and in breccia clasts indicate that plagioclase or aluminum-rich basalts are a common component of the pre-mare lunar surface.

- 3) The 2.4-m core tube shows that the lunar regolith probably contains a substantial stratigraphic history.

- 4) An unusual green glass component, rich in the soil samples from the front, suggests that in the vicinity of this site there is a rock type rich in magnesium and iron that has not been sampled at previous sites.

- 5) Most of the carbon found on the lunar surface was emplaced there by the solar wind.

- 6) Variations in the abundance of  ${}^{40}\text{Ar}$  in several soil samples further support the hypothesis that  ${}^{40}\text{Ar}$  may escape into the lunar atmosphere and be recaptured from this atmosphere.

## References and Notes

1. Apollo Lunar Geology Investigation Team, *Science* **175**, 407 (1972).
2. The members of the Lunar Sample Analysis Planning Team are A. J. Calio, M. B. Duke, A. L. Burlingame (University of California, Berkeley), D. S. Burnett (California Institute of Technology, Pasadena), B. Doe (U.S. Geological Survey, Denver, Colorado), D. E. Gault (NASA Ames Research Center, Moffett Field, California), L. A. Haskin (University of Wisconsin, Madison), W. G. Melson (U.S. National Museum, Smithsonian Institution, Washington, D.C.), J. Papike (State University of New York, Stony Brook), R. O. Pepin (University of Minnesota, Minneapolis), P. B. Price (University of California, Berkeley), H. Schnoes (University of Wisconsin), B. Tilling (NASA headquarters, Washington, D.C.), N. M. Toksoz (Massachusetts Institute of Technology, Cambridge), and J. A. Wood (Astrophysical Observatory, Smithsonian Institution). Those members listed with no institution are from the NASA Manned Spacecraft Center, Houston, Texas.
3. L. H. Ahrens and H. Von Michaelis, *Earth Planet. Sci. Lett.* **5**, 395 (1969).
4. Lunar Sample Preliminary Examination Team, *Science* **173**, 681 (1971).
5. M. H. Carr and F. El Baz, *U.S. Geologic Survey Map 1723* (U.S. Geological Survey, Washington, D.C., 1971).
6. G. D. O'Kelley, J. S. Eldridge, E. Schonfeld, P. R. Bell, *Geochim. Cosmochim. Acta* (Suppl. 2) **2**, 1747 (1971).
7. Lunar Sample Preliminary Examination Team, *Science* **165**, 1211 (1969).
8. C. B. Moore, E. K. Gibson, J. W. Larimer, C. F. Lewis, W. Nichiporuk, *Geochim. Cosmochim. Acta* (Suppl. 1) **2**, 1375 (1970).
9. K. Norrish and J. T. Hutton, *ibid.* **33**, 431 (1969).
10. K. Norrish and B. W. Chappell, in *Physical Methods in Determinative Mineralogy*, J. Zussman, Ed. (Academic Press, New York, 1967), p. 161.
11. KREEP (potassium, rare-earth elements, and phosphorus) is discussed by C. Meyer, Jr., R. Brett, N. J. Hubbard, D. A. Morrison, D. S. McKay, F. K. Aitken, H. Takeda, and E. Schonfeld [*Geochim. Cosmochim. Acta* (Suppl. 2) **1**, 393 (1971)].

# Genes Conferring Specific Plant Disease Resistance

Differences in behavior may reflect structure differences with important general implications.

K. W. Shepherd and G. M. E. Mayo

Although it is well known that major genes control the resistance of plants to a wide variety of parasites and that these genes are of value when producing resistant forms of crop plants (1), the detailed structure and function of these host genes remain obscure. For example, it has frequently been reported that genes conferring resistance to an obligate parasite are grouped together in a small segment of a host chromosome, but in most cases it is not known whether these genes are closely linked or functionally allelic.

One of the best examples of such groups of host genes comes from the work of Flor (2) with flax (*Linum usitatissimum* L.) and its rust [*Melampsora lini* (Ehrenb.) Lévl.] where genes dominant for conferring resistance have been assigned to five "loci" named *K*, *L*, *M*, *N*, and *P*, with 1, 11, 6, 3, and 4 "alleles," respectively. Other good examples include the *Rp<sub>1</sub>* locus in maize (*Zea mays* L.) and the *Mla* locus in barley (*Hordeum vulgare* L.), where 14 different genes conferring resist-

ance to maize rust (*Puccinia sorghi* Schw.) (3) and at least 7 different genes conferring resistance to powdery mildew (*Erysiphe graminis* D.C. f.sp. *hordei* E. M. Marchal) (4) have been identified, respectively.

Initially, the genes within these groups were considered allelic when they failed to show recombination among *F<sub>2</sub>*, *F<sub>3</sub>*, or a limited number of testcross progeny (5). Recently, however, more critical data on the structure of some of these groups have been obtained by testing much larger testcross families.

For example, both Flor (6) and Shepherd (7) detected rare recombination between genes from each of the *L*, *M*, and *N* groups in flax. In the more extensive studies of Flor, the expected reciprocal products of recombination were recovered with the *M* and *N* genes, but only the double recessive phenotypic class was detected with the *L* genes tested. Also, Saxena and Hooker (3) showed that several of the genes in the *Rp<sub>1</sub>* group of maize could be recombined with low frequency and reciprocal products were recovered whenever the testcross progeny were tested with an appropriate combination of rust strains.

From these results it was concluded that each of the *M*, *N*, and *Rp<sub>1</sub>* groups are complex regions of chromosome possessing several closely linked genes that can be recombined reciprocally (3, 6). Because the reciprocal products of recombination were not detected with *L* genes, Flor was unable to decide whether these genes are "mutually exclusive alleles" or closely linked genes. However, we shall show that when his results are compared with the expectations from a modified *cis-trans* test for allelism, the *L* genes appeared to behave as functional alleles.

In our work we have set out to test critically the possibility that some groups of genes conferring disease resistance consist of closely linked genes, whereas others consist of a series of functional alleles. The practical importance of deciding between allelism and close linkage has been stated by other workers (3, 6), but such a decision could contribute to an understanding of the origin and mode of action of genes conferring disease resistance. Consequently we have chosen flax and its rust to make a detailed study of recombination between two gene groups, *L* and *M*, that seem to have different structures. Our results are reviewed in this paper and more detailed treatments are forthcoming (8, 9).

## Concept of Allelism and a Modified Cis-Trans Test

Before referring to our experiments, it is necessary to choose an operational definition of the gene, and hence allelism, appropriate for genes controlling disease resistance. The modern definition of the gene is as a unit of function, the cistron, which has been shown to be composed of numerous mutant sites separable by recombination [see, for example, Fincham (10)]. Thus to

Dr. Shepherd is senior lecturer in the department of agronomy at Waite Agricultural Research Institute. Dr. Mayo is senior lecturer in the department of genetics at the University of Adelaide, North Terrace, Adelaide, South Australia 5001.